VCU

Virginia Commonwealth University

VCU Scholars Compass

Theses and Dissertations

Graduate School

2020

Generation of Warm Dense Plasma on Solar Panel Infrastructure in Exo-Atmospheric Conditions

Harrison C. Wenzel
Virginia Commonwealth University

Follow this and additional works at: https://scholarscompass.vcu.edu/etd

Part of the Dynamics and Dynamical Systems Commons, Mechanics of Materials Commons, and the Semiconductor and Optical Materials Commons

Downloaded from
https://scholarscompass.vcu.edu/etd/6153

Generation of Warm Dense Plasma on Solar Panel Infrastructure in Exo-Atmospheric

Conditions

By

Harrison Cole Wenzel

Thesis

Submitted for the fulfillment of

Master Degree in Nuclear and Mechanical Engineering

Virginia Commonwealth University

Richmond, Virginia

Advisor:

Dr. Gennady Miloshevsky

Mossi. Also, I would like to thank my research partner and dear friend, Myles Fogleman. Our work was at times very difficult and tedious, having you there to keep me motivated and to work on the problems at hand was invaluable. In the acknowledgments section of your thesis you wrote," I am proud to say that coming out the other end of this process I will leave with a degree as well as a new friend." I am also proud to call you a friend.

Finally, I would like to thank my girlfriend, Erin Tyra. Erin, the love and support you have had for me over the past few years has been incredible. The fact that I can always count on you to be there for me has changed my life in so many ways for the better. Thank you for sticking with me and helping me pursue my dreams. There is no way that I could have done this without you. I love you.

Abstract

The use of a weaponized thermo-nuclear device in exo-atmospheric conditions would be of great impact on the material integrity of orbiting satellite infrastructure. Particular damage would occur to the multi-layered, solar cell components of such satellites. The rapid absorption of X-ray radiation originating from a nuclear blast into these layers occurs over a picosecond time scale and leads to the generation of Warm Dense Plasma (WDP). While incredibly difficult and costly to replicate in a laboratory setting, a collection of computational techniques and software libraries may be utilized to simulate the intricate atomic and subatomic physics characteristics of such an event. Use of the Monte Carlo sampling method within the *Geant4* software library allows for the energy deposition and power density profiles by X-rays into this system to be determined. By understanding and modeling the different factors which can affect the absorption of thermonuclear X-ray radiation, specifically, "cold –X-ray radiation," in the energy range of approximately 1 to 1.5 keV, the molecular dynamics modeling of WDP generation and evolution can be performed using the *LAMMPS* code library. One aspect modeled and utilized within this software is the Planck blackbody spectrum of X-rays, assumed to be emitted by the detonation. Another such factor explored is the effect of primary and secondary particle backscattering within the active solar cell layer. Ultimately, it was determined that the primary and secondary particle backscattering of photons and electrons occurs at such a relatively low rate that its effect on the properties of the generated WDP is negligible. Once the energy deposition and power density profiles are determined, *LAMMPS* is utilized in order to understand the spatio-temporal evolution of the WDP as well as the temperature, stress, and mass density distribution within the material, at its surface, and its immediate vacuum surroundings.

Table of Contents

Introduction

The detonation of a thermonuclear device beyond earth's atmosphere would have catastrophic consequences to orbiting satellite infrastructure, specifically the solar panels aboard such systems. A primary radiation emitted in such a detonation event, resulting in the surface damage of materials will take the form of low energy X-rays within an energy range from about 1 to 1.5 keV. X-ray photons within this energy range are denoted as, "cold" photons due to their relatively low energy range.

This work examines how damage to the sensitive solar cell components of a satellite device is incurred while exposed to cold photons during an exo-atmospheric nuclear detonation event. One element of specific interest is the rapid formation of Warm Dense Plasma (WDP) that occurs on the material's surface during cold photon exposure.

While there exists historical records of sensitive electronic devices becoming damaged during exposure to radiation from a thermonuclear event (such as the STARFISH PRIME test) [1], as well as physical lab equipment able to generate photon beams (such as the Linac Coherent Light Source) analysis of the system in question requires a different approach. Because the use of physical beam generators in a laboratory setting are highly resource intensive and unable to perfectly recreate the conditions present during exo-atmospheric exposure to a thermonuclear weapon, computer simulation techniques are employed. By using software tools such as *Geant4* and *LAMMPS*, the irradiation of solar cell targets via cold photon exposure can be simulated and analyzed. *Geant4* is an open source toolkit utilized and developed by CERN in order to further the study of atomic and subatomic particle interaction. *LAMMPS* is an open source software library developed and maintained by Sandia National laboratory. By using these two tools in concert, a simulation in which a specified target geometry is generated and irradiated can be

developed within the *Geant4* environment and then the molecular dynamics (MD) of such a system can subsequently be analyzed via the use of *LAMMPS*.

By developing code-sets based on the *Geant4* and *LAMMPS* software libraries, the simulation of satellite exposure could occur without the need for expensive and impractical lab equipment. By simulating the complex physics that occurs during cold photon exposure onto the solar cell infrastructure of orbiting satellites, a better understanding of how the damage onto these structures occurs due to the rapid generation of WDP was ultimately achieved.

Physical Phenomena and WDP generation

1.1 Warm dense matter

Warm dense plasmas comprise the largest fraction of the WDM regime. The WDM regime is understood to exist within a range of temperatures ~1 - 100 eV. The densities of the WDM regime range in scale from 10^{-2} to 10^4 g/cm^3, of this range the WDP sub regime may be comprised of densities from 1 up to 10^4 g/cm^3 [2]. A phase diagram illustrating the WDM regime in relation to other states of matter is shown in **Fig 1**.
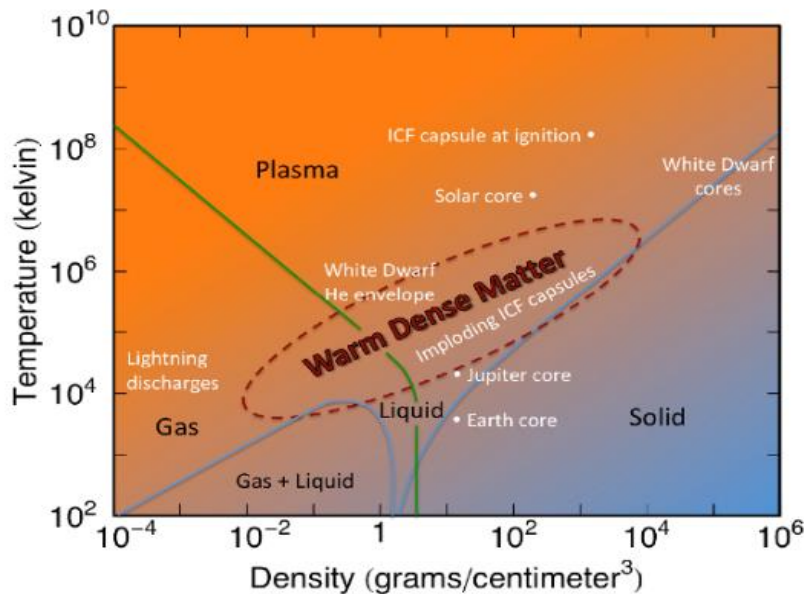
Fig 1: Warm dense matter phase diagram [2]

While WDP comprises the majority of traditional matter in the universe it is very difficult to generate in a laboratory setting [3]. WDPs may exist in a stable form inside the deep interiors of large exoplanets, a significant amount of energy must be provided by a device such as the Linac Coherent Light Source (LCLS) X-ray laser in order to rapidly generate WDP [4]. The WDP is created due to the immense amount of heat (~20,000 K) and pressure (~4.5 Mbar) generated by the LCLS X-ray laser device onto an ultrathin aluminum film [4]. Exposure to this

high energy X-ray beam causes changes to the systems Coulomb coupling parameter and quantum degeneracy parameter, ultimately yielding the WDP.

1.2: Coulomb coupling / Quantum degeneracy parameters

In order to achieve a better sense of the underlying physics behind WDP generation it is important to utilize a theoretical framework. Because the WDM regime exists at the intersection of classical plasma physics and condensed matter quantum mechanics an analysis of the WDP system must take both paradigms into consideration. Although the underlying mathematics behind both classical and quantum plasma physics are highly complicated, a fundamental understanding of what is theoretically occurring within the WDM regime can be gained by analyzing Coulomb coupling parameter (Γ) of classical plasma physics and the quantum degeneracy parameter (θ) of quantum mechanics.

The Coulomb coupling parameter is understood to be the ratio of a materials mean potential energy per particle to the materials mean kinetic energy per particle. This definition is given in the following equation:

$$\Gamma = \frac{E_{potential}}{E_{kinetic}}$$

Where Γ is the Coulomb coupling parameter, $E_{potential}$ is the mean potential energy per particle, and $E_{kinetic}$ is the mean kinetic energy per particle. The value of the Coulomb coupling parameter determines the ease with which particles may move throughout the system. Fluid systems have Coulomb coupling parameters much less than 1 (with a theoretical ideal gas having a Coulomb coupling parameter of $\Gamma = 0$) as particles within these systems may easily move past

one another due to the low amount of coupling. This ability is not observed in systems with

Coulomb coupling parameters much greater than 1 due to the high degree of particle coupling.

Within the field of Quantum Mechanics the quantum degeneracy parameter is understood

to be the ratio of a system's thermal energy to its Fermi energy. This relationship is given in the

following equation:

$$\theta = \frac{k_b T}{E_f}$$

Where θ is the quantum degeneracy parameter, $k_b T$ is the thermal energy of the system, and E_f

is the Fermi energy. When the quantum degeneracy parameter is much greater than 1, the system

may be considered non-degenerate. In this non-degenerate state quantum mechanical effects may

be ignored. If this parameter is much less than 1 however the system is considered to be

degenerate and quantum effects must be taken into consideration when characterizing the

fermionic nature of the system's electrons.

Both the classical and quantum frameworks used to describe plasma materials break down as both the Coulomb coupling parameter and the quantum degeneracy parameter approach a value equivalent to 1. It is at this interface, between the quantum and classical regimes, that WDM occurs. A graphic illustrating this point of interest may be seen in **Fig 2**.
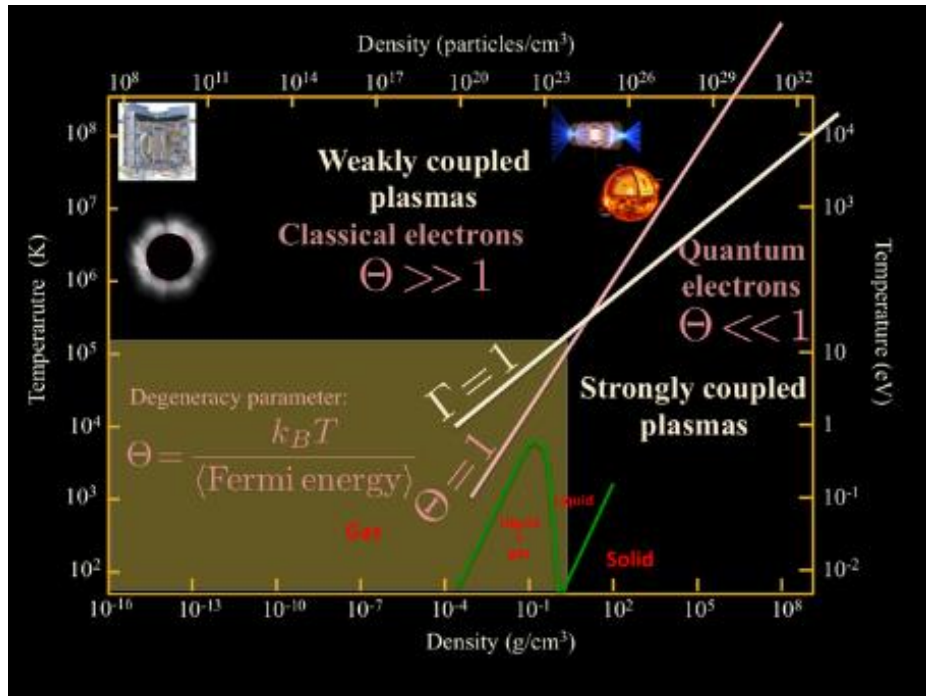
Fig 2: Point of coupling and degeneracy parameter unity [5]

The point of coupling and degeneracy parameter unity causes theoretical frameworks to break down. Because of the breakdown in both the classical and quantum frameworks, techniques such as Monte-Carlo modeling must be utilized in order to gain insight into the properties of WDM [5].

As a target material is exposed to X-ray radiation, various subatomic, physical phenomena may

occur resulting in damage to satellite infrastructure and the generation of WDP. Two particularly

noteworthy subatomic events that occur during X-ray exposure are photoabsorption and

Compton scattering.

As an energetic photon enters a target material there exists a probability that it collides

with an electron within the material. Due to the physical conservation laws of momentum and

energy, when such a collision occurs, the electron enters a state of recoil while the initial photon

is deflected into a lower energy state. This reduced energy, deflected photon will also have a

longer wavelength in accordance with the Planck-Einstein relationship. The scattering of

secondary electrons due to incident photon radiation within a given target material is a

phenomenon known as Compton scattering. An illustration of Compton scattering is provided in

Fig 3 [6].

Fig 3: Compton scattering [6]

Photoabsorption refers to the process by which photons are absorbed into an atom within

a target material, forcing that atom into an excited energy state. Once an atom enters an excited

energy state due to photoabsorption it may then eject a secondary photoelectron in order to return

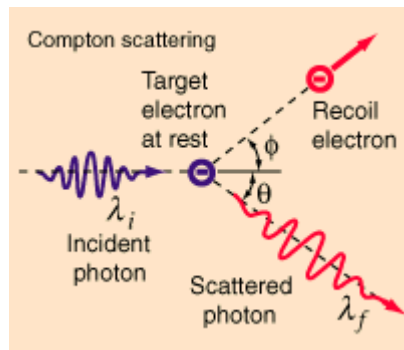to the previous unexcited state. Understanding the process of photoabsorption is critically important within the context of this research as the point of photoabsorption is the final point of a photon's trajectory within the target material. If photoabsorption does not occur during the particle history, the photon has escaped the target system via backscattering.

Because photoabsorption occurs at points of collision between the incident photons and target atoms within a given material it is necessary to calculate the collision density of a given system. The collision density is understood to be in terms of collision per unit volume and unit time (collisions / $cm^3 \cdot s$). The collision density is calculated via the following equation:

$$F = I\Sigma$$

Where F is the collision density, I is the photon intensity, and Σ is the target's macroscopic cross section. Both the photon intensity and macroscopic cross section can be calculated via the following equations:

$$I = I_0 e^{\Sigma z}$$
$$\Sigma = N\sigma$$

Where I_0 is the initial photon intensity, z is the depth into the material, N is the material's atomic number density, and σ is the microscopic cross section of the material [7].

Over the course of a photon's trajectory a combination of Compton scattering and photoabsorption may occur. As the X-ray beam is incident upon a target material, photons may deflect multiple times throughout the system via Compton scattering ultimately exiting the

system (backscattering) or being absorbed into the target material itself (photon absorption). One statistic of interest to this research is the ratio of backscattered primary photons and secondary electrons to the total number of simulated photon histories. **Fig 4** illustrates the difference between the two ultimate results of a photon's trajectory.
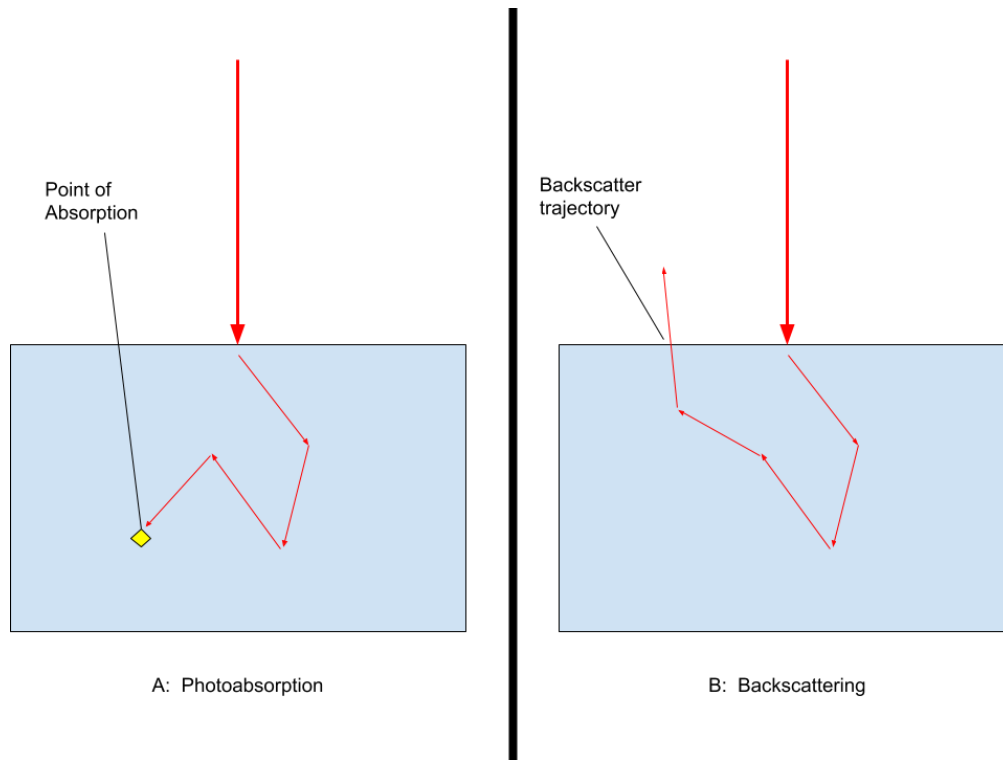

Point of Absorption

A: Photoabsorption

Backscatter trajectory

B: Backscattering

Fig 4-A: Photon trajectory ending in photoabsorption

Fig 4-B: Photon trajectory ending in backscattering

System Modeling

2.1: Monte-Carlo / Geant4

Monte-Carlo simulation techniques are utilized as a means to simulate the numerous rapid particle interactions which occur at the point of material exposure to oncoming radiation. The, "Monte-Carlo method," gains its name from the fact that, at the most fundamental level of any Monte-Carlo code, the use of random number generation is essential. By inputting system properties such as the initial energy of the incident beam; oncoming particle type and charge; material properties of the target such as target composition, and density; and other related physical attributes of the system under study. Incorporating these physical properties into the software allows for the calculation of different probabilities of various physical phenomena occurring, including particle scattering and absorption. By combining these calculated probabilities with the use of random number generation, an acceptable model can be produced.

A major caveat with regards to the use of Monte-Carlo modeling techniques is in the fact that a large number of particle histories are required in order to assure the accuracy of a given simulation. The utilization of a considerable amount of particle histories is very resource intensive as the simulation of each particle requires the recalculation of different scattering and absorption probabilities at various points throughout the particle's trajectory into the target material. It should be noted that in the event of an actual exo-atmospheric, thermonuclear event the number of photons radiating a satellite target would be upwards in the order of trillions of individual particles. While it is not practical to simulate this magnitude of particle histories with anything less than a supercomputer, accurate results may still be attained. The level of simulation accuracy with respect to the number of particle histories may be observed in the use of history

normalization in results. An example of the use of particle history normalization is seen in the formula for simulation variance:

$$\sigma^2 = \frac{1}{N}$$

In the above formula σ^2 is the simulation variance (deviation from the mean) and N is the total number of particle histories performed during the Monte-Carlo simulation. The inverse relationship exemplified here also allows for the comparison of results between publications as different number of particle histories may be performed. The use of particle history normalization will be evident in the results section of this paper.

The *Geant4* simulation toolkit was used in tandem with custom developed codesets in order to accurately simulate the conditions present during satellite infrastructure radiation via exo-atmospheric thermonuclear detonation. *Geant4* is a set of libraries and tools written in C++ that is currently in active development at CERN and other collaborating laboratories. It is described as," a toolkit for the simulation of the passage of particles through matter. Its areas of application include high energy, nuclear and accelerator physics, as well as studies in medical and space science." [8] As such, Geant4 is an excellent platform for this work as it allows for the input, customization, and manipulation of various system parameters. One of these relevant system parameters is the construction of the target geometry itself.

2.2: System Geometry

The solar cell infrastructure present in satellites orbiting beyond the Earth's atmosphere can be understood as an ordered sequence of layered slabs. Individual stacks of these layered slabs are then attached to a Kapton substrate. The active elements of each stack are then wired together via an interconnecting cable. **Fig 5** illustrates this geometry.
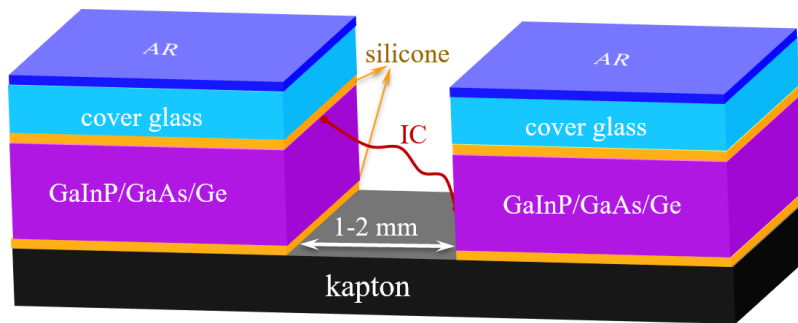
Fig 5: Solar cell geometry [9]

The 1-2 mm gap present within this geometry leaves the side portions of each slab exposed to the vacuum of space. In the case of an exo-atmospheric thermonuclear event, this exposed design will lead to direct X-ray bombardment of the active GaInP/GaAs/Ge layer.

The active semiconductor GaInP/GaAs/Ge layer is of great importance to the system as it is the element responsible for the primary generation of electricity. Severe damage to this region of the satellite's solar cell infrastructure would lead to circuit shortages and other catastrophic failures. This layer is comprised of 3 sub-layers, the topmost is a 0.8μm, Gallium-Indium-Phosphide layer; a 3.6μm, Gallium-Arsenide middle layer; and a 300μm, Ge bottom layer. An illustration of these subdivisions can be seen in **Fig 6.**
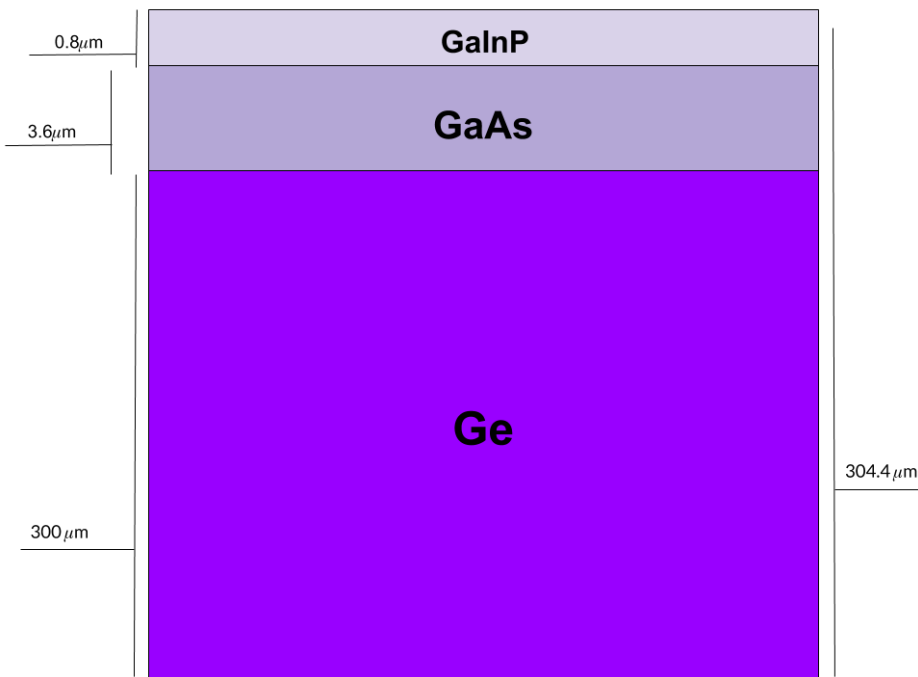
Fig 6: Active semiconductor layer subdivisions (Not to scale)

It is evident from **Fig 6** that the Ge sub-layer comprises the relative majority of the active

component of the solar cell geometry. Because of the active semiconductor component's

importance to the overall satellite infrastructure, it is necessary to perform Monte-Carlo and

Molecular Dynamics simulations using it as the target geometry. Since the Ge sub-layer

comprises 98.5% of the total active layer and its modeling is relatively straightforward using

both the *LAMMPS* and *Geant4* toolkits, a Ge target was constructed for both the *Geant4* and

LAMMPS code-sets.

Along with the physical composition of the target itself, the distance between the

thermonuclear event and the target must be taken into consideration. There exists a geometric

attenuation factor that must be utilized when calculating the power density and energy deposition

profiles caused by cold photon exposure onto the target material. The inverse square formula for this factor is as follows:

$$F = \frac{R^2}{D^2}$$

where F is the geometric attenuation factor, and D is the distance between the target and explosion (in terms of cm) and R is the radius of the explosion's fireball. For the purposes of this research a distance of 100 kilometers and a radius of 1 meter is assumed to be present between the target and the detonation event These values yield an F value of 10^{-10} [9].

2.3: Planck Blackbody Distribution

The Monte-Carlo code-set is designed to be able to simulate exposure from either a monoenergetic particle beam or one based on a blackbody spectral distribution of X-rays. Although the exact energy spectrum emitted by a thermonuclear weapon is classified information, it can be reasonably assumed that this spectral distribution is highly similar to that of a Planck blackbody. In order for the primary generated beam particles to have energies determined by a blackbody energy distribution, the Planck function must be properly incorporated into the code-set. In terms of frequency, this function is understood to be:

$$\frac{dN(\upsilon, T)}{d\upsilon} = \frac{2\pi\upsilon^2}{c^2} \frac{1}{exp(h\upsilon/kT) - 1} \left[\frac{1}{cm^2 \cdot s \cdot Hz}\right]$$

In this function υ is representative of the photon's frequency while T represents the spectrum's temperature in units of Kelvin. The physical constants in this equation are understood to be: Planck's constant, h, is equivalent to $4.1356677 \times 10^{-18}\ keV \cdot S$; the speed of light, c,

is equivalent to 2.99792458×10^8 m/s; and Boltzmann's constant, k, is equal to 1.380649 $J/$ K. Because of the Planck-Einstein relation, $\varepsilon = hv$, the Planck function may be rewritten in terms of photon energy.

$$\frac{dN(\varepsilon, T)}{d\varepsilon} = \frac{2\pi\varepsilon^2}{c^2 h^3} \frac{1}{exp(\varepsilon/kT) - 1} \left[\frac{1}{cm^2 \cdot s \cdot keV}\right]$$

The performance of numerical integration via the use of Gaussian quadratures allows for the relationship between photon energy and photon flux to be determined. Numerical integration was performed on the following function:

$$N(\Delta\varepsilon_i, T) = \frac{2\pi}{c^2 h^3} \int_{\varepsilon_i}^{\varepsilon_{i+1}} \frac{\varepsilon^2}{exp(\varepsilon/kT) - 1} d\varepsilon \left[\frac{1}{cm^2 \cdot s}\right]$$

After having generated flux and energy arrays, a probability density function was generated. This probability density function, combined with Monte-Carlo sampling techniques, enabled the primary beam generation to follow the properties of a blackbody. Ultimately, the properties of this generated beam could be numerically verified via comparison to the net photon flux equation:

$$F_{ph} = \frac{4\pi\xi(3)}{c^2 h^3} k^3 T^3 \approx 2.38 \times 10^{32} \left[\frac{ph}{cm^2 \cdot s}\right]$$

Where the blackbody temperature has been set and Apery's constant, $\xi(3)$, is approximately equal to 1.20205 [1].

2.4: Primary / Secondary backscatter implementation

The Geant4 toolkit allows for the simulation of an extensive list of sub-atomic particle interactions. Phenomena of primary concern when considering cold X-ray bombardment onto the active semiconductor, target geometry include Compton scattering and photon absorption. Code-sets developed within the Geant4 environment can be used to track particles as they enter the target geometry and are scattered and/or absorbed. An initial concern of this research questioned whether primary or secondary particle backscattering would have any effect on the generation of WDPs in the exo-atmospheric environment. Primary particles being the initial cold X-rays emitted during explosion, while secondary particles are the electrons contained within the target geometry at the time of exposure.

While backscattered particle yield was the primary metric under consideration when performing the system backscatter experiments, another statistic of interest was particle escape angle relative to the slab surface. At the time of initial investigation, it was theorized that if the particle yield were significant enough to have a possible effect on WDP generation it would be necessary to know in which direction these particles were exiting the target geometry. Implementation of backscattered particle tracking into the Geant4 code-set allowed for the escape angle of the analyzed particle relative to the normal vector of the target surface to be obtained. These angles were then understood as angle cosines in the range from 0 (parallel to target surface) to 1 (perpendicular to target surface). A diagram of this setup is shown in **Fig 7.**
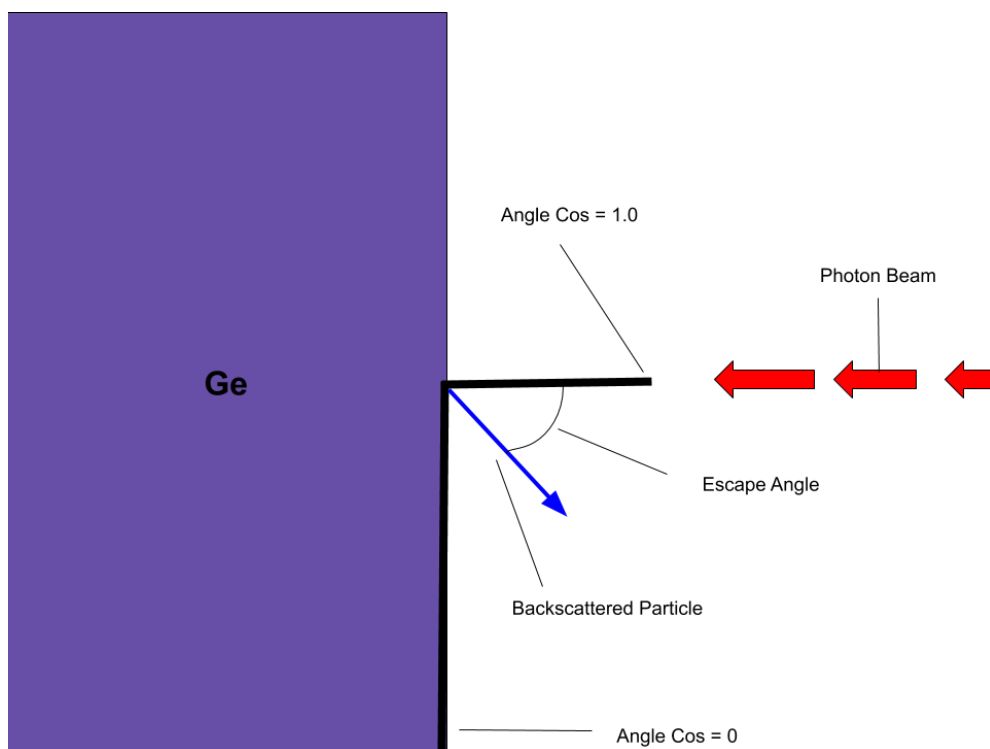
Fig 7: Illustration of backscatter particle escape angle tracking.

With the set up illustrated above in **Fig 7** and the implementation of escape tracking with the Geant4 code-set, the normalized particle yields of backscattered primary photons and secondary electrons could be determined. This combined with the knowledge gained from analysis of the angle of backscattered particle escape would allow for a greater understanding of the net effects of the subatomic, scattering and absorption phenomena occurring within the target at the time of X-ray exposure and WDP generation.

2.5: Interatomic potential

Molecular dynamics (MD) simulations are utilized to simulate the set of particles and their properties over a pre-determined time interval. MD simulations are fundamentally constructed on the concept of interatomic potentials. Within the defined collection of atoms in an MD simulation, there exists a potential energy function (V) from which the force applied to each particle, individual particle trajectory, and ultimately the properties of the entirety of the system can be derived. This interatomic potential is, itself, a function of the relative positions within space. The force exerted upon a given i^{th} particle can be characterized as follows:

$$F_i = -\nabla V(r_1, r_2, \ldots, r_N)$$

where $-\nabla V$ is the change in potential energy over a given timestep, r_j is the physical coordinates of a given particle, and N is the number of particles within the MD model. This idea can be derived from the understanding that an MD simulation is comprised of the interactions of nuclei and electrons within a set space. The application of the Born-Oppenheimer approximation, which states that because nuclei are significantly more massive than electrons they move ~100 times slower and can be regarded as fixed relative to electron motion. With this approximation, the problem can be understood in terms of the total wave function:

$$\Psi(R_i, r_n) = \Xi(R_i)\Phi(r_n; R_i)$$

where Ξ refers to the nuclei and Φ contains the electron information. This system can be further broken down into a collection of two separate Schrödinger equations. This quantum system becomes extremely resource intensive to solve however and is replaced in favor of a chosen set of analytical formulas as to mimic the realistic behavior of the interatomic potential. One such collection of analytical formulas is defined in the family of Tersoff potentials.

The Tersoff potential was utilized within this body of work in order to perform the appropriate MD simulations concerned with the ablation of the Ge target due to X-ray radiation. The Tersoff interatomic potential is defined as:

$$V = \frac{1}{2}\sum_{ij}\phi_R(r_{ij}) + \frac{1}{2}\sum_{ij} B_{ij}\phi_A(r_{ij})$$

where R and A refer to the repulsive and attractive forces comprising the pair potential. The B term refers to the bond order of particles i and j. The presence of this bond order term increases the complexity of this interatomic potential model significantly as it determines how bonds between any two atoms are weakened due to the presence of any additional inter-atomic bonds in which either of the two atoms within the bond take part in [10].

2.6: MD property calculations

By utilizing the Tersoff potential within the MD simulation, data on the physical properties of the system can be generated and collected. Generation of this data requires the use of a defined, "supercell." Simply put these "supercells" are numbered collection of particles within the entire system itself. The data generated within this report used supercells comprised of 2,000 Ge atoms.

The temperature of the system was simulated over a temporal evolution of 10 ps. After each timestep the average kinetic energy of a supercell is determined with the following formula:

$$T = \frac{1}{2}mv^2$$

where m is the atomic mass of Ge and v^2 is the square of the average velocity of the atoms within the supercell. The internal stress is calculated in a similar manner by tracking the average force per cross sectional area within a supercell. Finally, the number of atoms within a supercell are counted and divided by the volume in which they inhabit to determine the atomic density.

LAMMPS is an acronym which stands for Large-scale Atomic/Molecular Massively Parallel Simulator [10]. *LAMMPS* is a MD simulation toolset developed and maintained by Sandia national laboratory. MD simulations are applicable to many fields of study that require the tracking and visualization of atomic and molecular scale particles during a simulated spatio-temporal evolution. Along with particle tracking, the tools present within the *LAMMPS* software library allow for code-sets to be developed that allow for the determination of other physical properties including, but not limited to, system temperature, stress, and mass density distribution.

The abilities afforded by the *LAMMPS* development environment make it a prime candidate for use in the analysis of WDP generation during solar infrastructure exposure to photon radiation. The code-set developed within this environment works in concert with results obtained from *Geant4* to generate the spatio-temporal evolution of the system as well as the physical properties of interest. This code utilizes the power density output of a given simulation that is obtained via the *Geant4* based simulation. A three-dimensional lattice array is then defined within the code-set to generate the target structure. In the case of the Ge, active semiconductor layer a diamond lattice was utilized with a lattice parameter of 5.658 Angstroms [11]. From here, other parameters of the simulation can be specified and manipulated such as the fraction of molecules generated in visualization output files (this aids in making the visualizations less resource intensive on system GPUs) as well as the number and value of timesteps between each output. Execution of the MD simulation results in the generation of .xyz files and .dat files. These .xyz files contain the Cartesian coordinate information of a collection of specified atoms at a given timestep. These files can then be illustrated with the use of PyMol visualization software. The .dat files contain three-dimensional data relating time, system depth,

and a physical property such as system temperature or mass density. These files can be plotted

using graphing software to generate three dimensional maps.

Results

3.1: Yield of Electrons and Photons

A 10 keV monoenergetic flux of X-ray's at normal incidence to the target surface was simulated in order to quantify the angular distribution and yield of backscattered primary photons and secondary electrons during active cell exposure. It was determined that the net yield of backscattered primary photons was $3.3x10^{-5}$% while the yield of backscattered secondary electrons was $1.6x10^{-5}$. These yields are very low relative to initial hypotheses and would suggest that electron and photon backscattering have little to no effect on the generation of WDPs.

The energy values with which primary, backscattered photons escaped the target system are displayed in **Fig 8**.
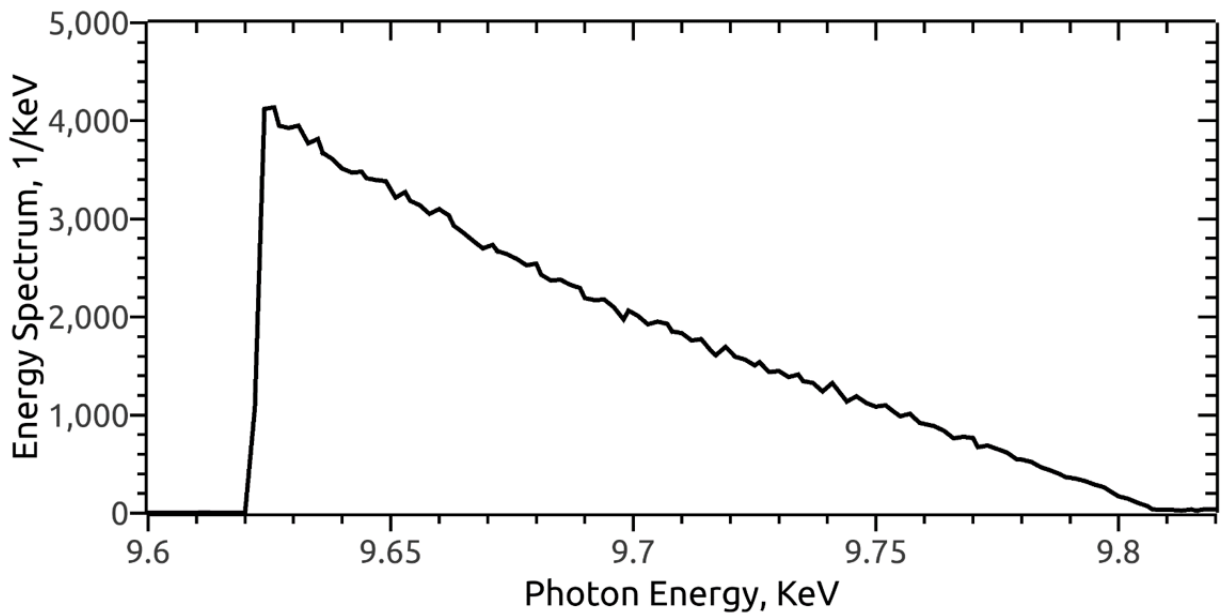

Fig 8: Photon escape energies in backscatter simulation

It can be clearly seen in **Fig 8** that the energy distribution of the backscattered photons is confined within the range between 9.62 keV and 9.82 keV. A majority of photons escaped with an energy approximately equal to the peak value at 9.62 keV with a downward linear trend to the highest escape energy value within the range of 9.82 keV.

The escape energy profile for the secondary electrons within this simulation is shown below in **Fig 9**.
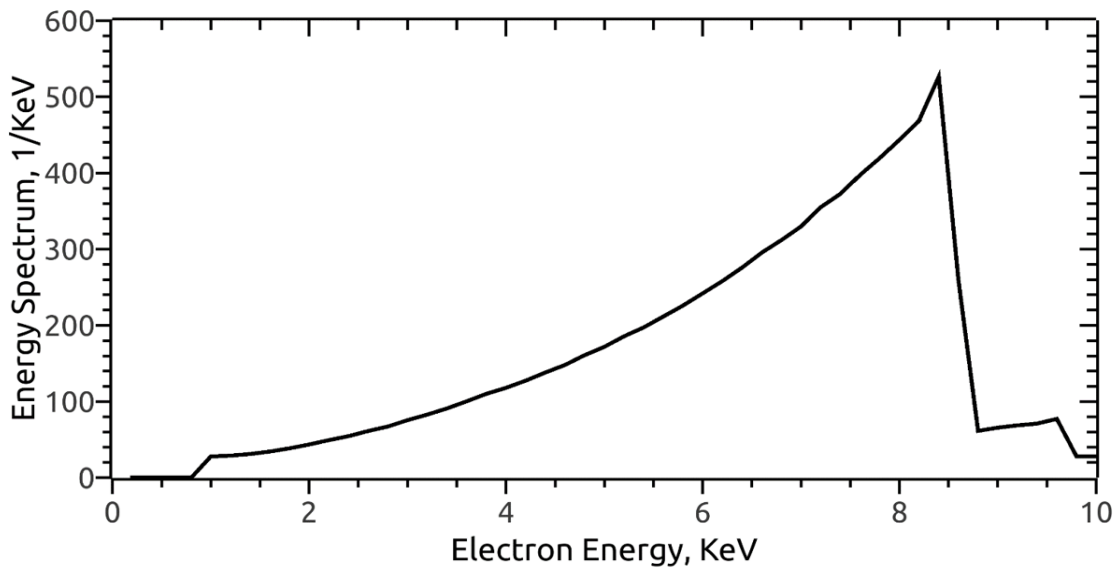

Fig 9: Electron escape energies in backscatter simulation

The energy range of escaped electrons is much wider compared to the escape energies of backscattered photons. **Fig 9** clearly illustrates the 1 to 10 keV escape energy range of the secondary electrons. An interesting result seen in Fig. 9 is the steep drop present after the peak escape energy value at approximately 8 keV.

The angular distribution of escaped photons and electrons is compared in **Fig 10**.
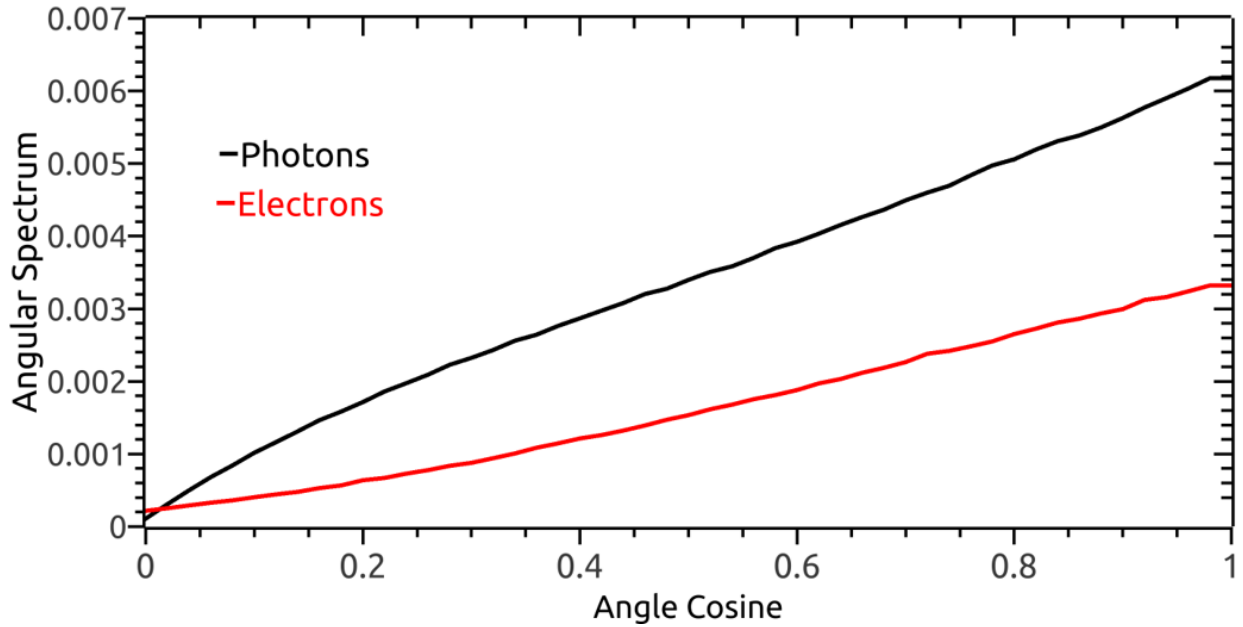

Fig 10: Photon and electron angular escape distributions

It is evident in **Fig 10** that for both primary photons and secondary electrons, the likelihood of backscatter escape increases linearly as the angle of escape approaches the normal (angle cosine = 1). The same is true for the flux of both the backscattered photons and the backscattered electrons.

3.2: Power Density Profiles

Analysis of the power density - allows for the understanding of where, and at what rate, energy is being deposited into the target system. As previously mentioned in Section 2.2 a geometric attenuation factor of 10^{-10} is considered when calculating the power density profiles. **Fig 11** shows a comparison of the power density curves for a 0.1 keV -, 1 keV -, and 10 keV temperature blackbody at normal X-ray incidence.
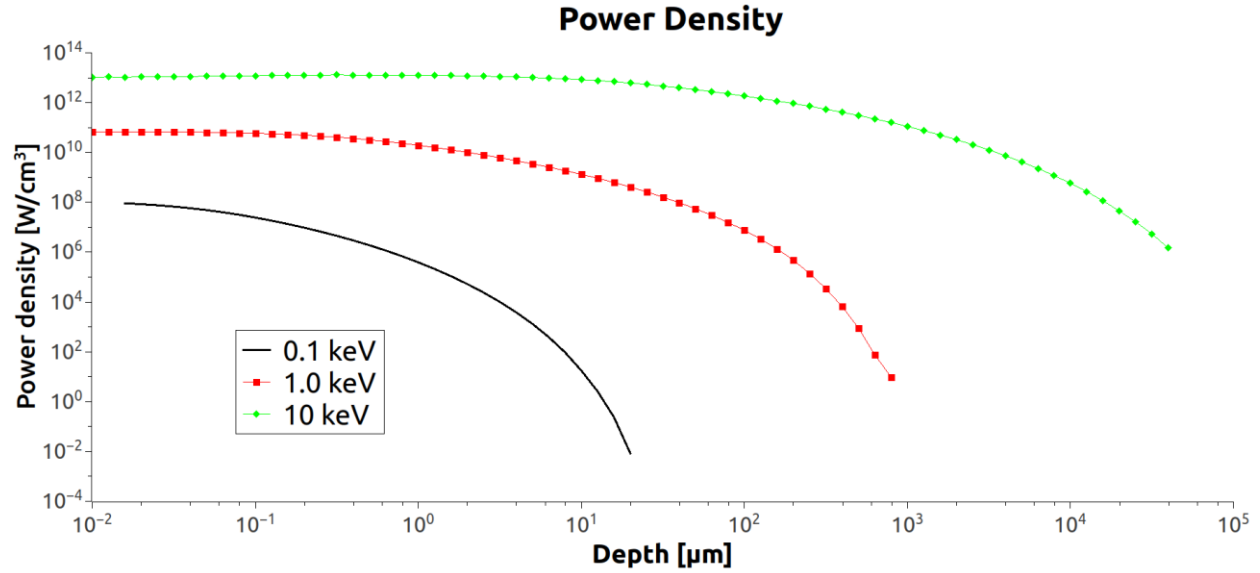
Fig 11: Power density vs. depth

Fig 11 displays the significant differences in the power density distribution from three blackbody spectrums with temperatures of increasing orders of magnitude. A 50 mm slab of Ge was used as the target within this collection of simulations. It is seen that X-rays have a varying amount of penetration depth into this slab, with energy being deposited to a depth of about 20 micrometers for the 0.1 keV X-rays and fully penetrating the slab for the 10 keV X-rays. The 0.1 keV X-rays have an initial dose rate on the order of $10^8 \ W/cm^3$ while the Y-intercept of the 10 keV case is on the order of $10^{13} \ W/cm^3$. The differences observed between these power density profiles become even more evident when analyzing the MD models of each respective simulation.

3.3: WDP Temperature, Stress, and Density

LAMMPS was used to predict temperature, internal stress, and density profiles for the case involving the exposure of the Ge active semiconductor target geometry to X-ray flux generated by the 0.1 keV blackbody spectrum. Color maps illustrating the front created by expulsion of the target material into space are shown in **Fig 12**.
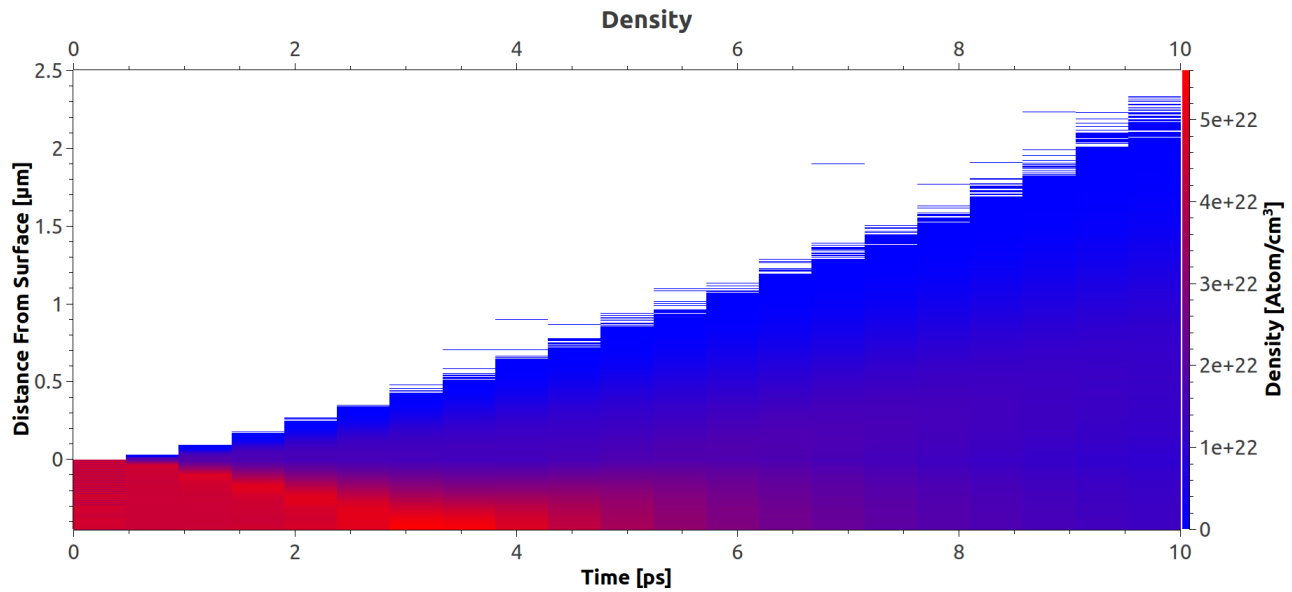

Fig 12-A: Map illustrating density of Ge target during exposure to a 0.1 keV temperature blackbody spectrum of X-rays
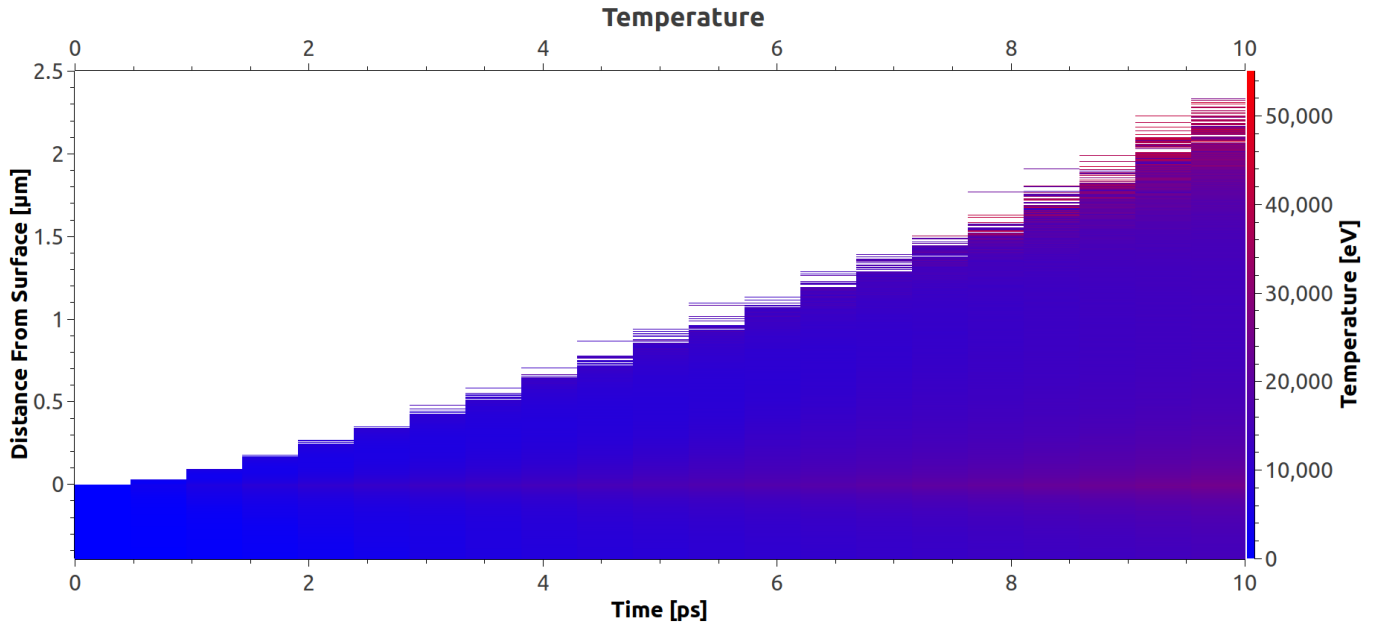
Fig 12-B: Map illustrating temperature of Ge target during exposure to a 0.1 keV temperature
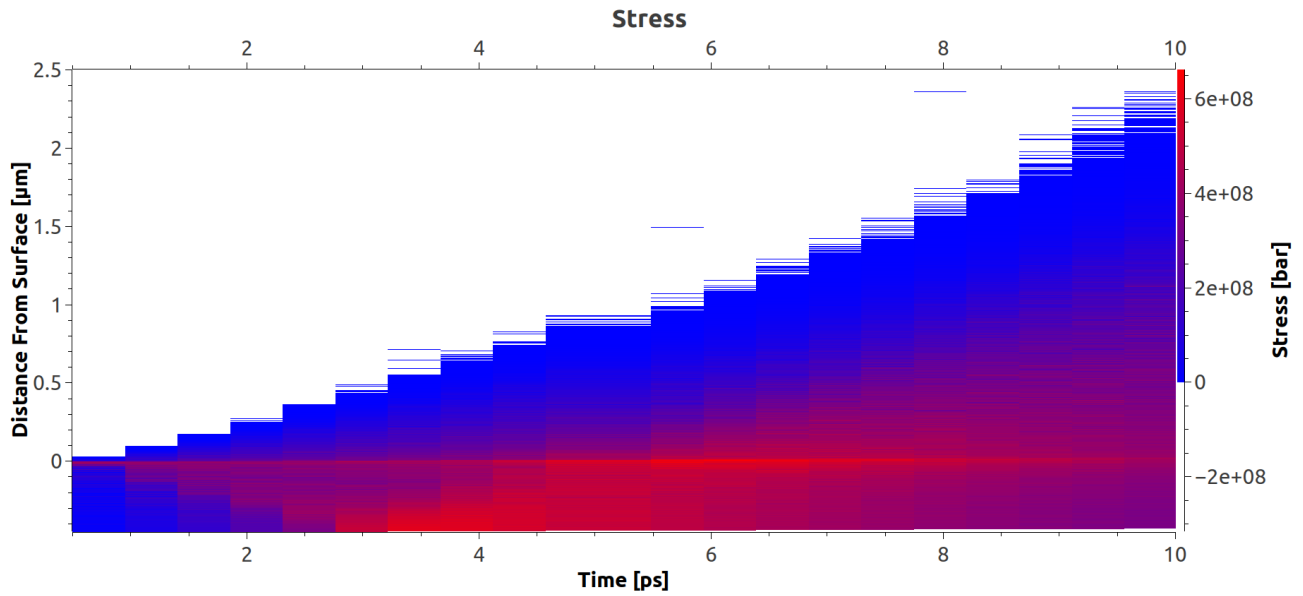
blackbody spectrum of X-rays

Fig 12-C: Map illustrating stress of Ge target during exposure to a 0.1 keV temperature

blackbody spectrum of X-rays

Periodic boundaries were used to define the lateral x and y boundary walls within the LAMMPS simulation used to generate **Fig 12**. The z-depth boundaries have utilized a non-periodic set up with a reflective boundary defined at the z-bottom. The target material had dimensions of 40 x 40 x 800 lattice parameters (226.3 x 226.3 x 4,526.4 Angstroms), a sufficiently large vacuum with a z dimension of 11,200 lattice parameters (63,369 Angstroms) was left above the surface of the target material to ensure that the ejected material undergoing expulsion could be properly analyzed. A time step of 1 femtosecond was defined with a net total of 1.0×10^4 time steps being analyzed, resulting in a 10 ps temporal evolution.

Fig 12 illustrates the expelled target material traveling a distance of ~2.3 micrometers after initial X-ray exposure. This low-density material front is comprised of plasma that can reach temperatures upwards of ~50 keV. Below this low-density plasma front is the WDP of interest. It is seen in **Fig 12** that the WDP regime exists from ~6 ps onwards with densities ranging from - 2×10^{22} and - 3×10^{22} atom/cm^3 and temperatures ranging in value from 1 to 100 eV. This region of WDP also appears to have relatively higher internal stress values as evident in **Fig 12-C**.

3.4: Spatio-Temporal Evolution of WDP

The MD simulation utilized to achieve the spatio-temporal mappings of system density, temperature, and stress was also able to generate a mapping of atom locations over the course of the simulated 10 ps evolution. In order to assure stability and preserve computational resources only a specified fraction (2%) of the ~10 million simulated atoms was traced throughout this 10 ps evolution. A diagram illustrating this mapping of particles at the 0.5, 2.5, 5.0, 7.5, and 10.0 ps timestamps is shown in **Fig 13**.

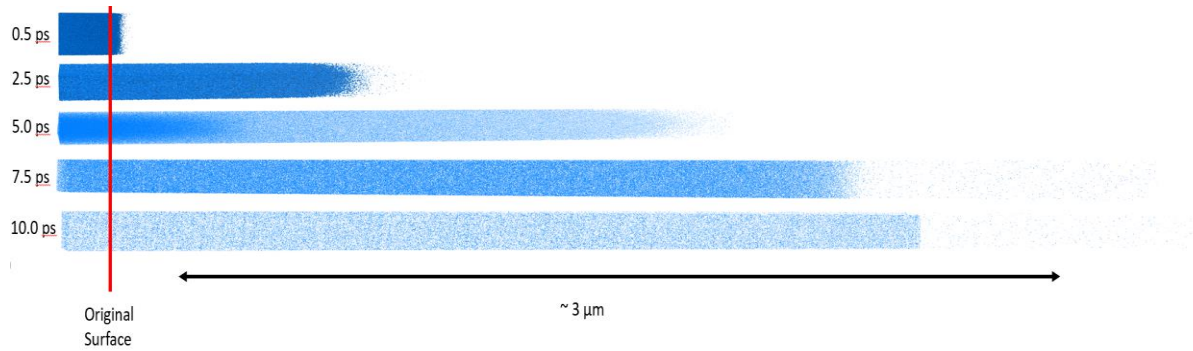**Fig 13**: Time-space atomic position mapping of the 0.1 keV blackbody X-ray exposure

The ejection of target material due to ablation into the vacuum of space is clearly observed to progress over the simulated 10 ps time scale. The visualization of the WDP material contrasts highly with the higher temperature, low density plasma observed to exist ~2.0 micrometers beyond the initial target surface.

Conclusion

The results on the backscattering suggest that the particle backscattering caused via the phenomenon of Compton scattering is of very little significance to the generation of WDPs within the target material. The low photon and electron yields, $3.3\text{x}10^{-5}\%$ and $1.6\text{x}10^{-5}\%$ respectively, observed in these simulations enables future work to continue without the need to account for particle backscattering and escape, freeing computational resources. Despite this fact it is still interesting to note that the majority of backscattered photons and electrons tend to escape with a trajectory parallel to the surface normal. Escaped photons range in energy from ~9.62 to 9.82 keV while escaped electrons have a wider energy range with energies ranging between 1 and 10 keV.

Analysis of the density, temperature, and stress profiles generated within LAMMPS illustrate the conditions in which WDP is generated during X-ray exposure of a slab of Ge. The destruction and expulsion of the target material within the vacuum of space generates the necessary prerequisites for the development of WDP near the original surface of the ablated target material. The WDP observed in the 0.1 keV simulation has density values ranging from $2x10^{22}$ and $3x10^{22}$ atom/cm^3 with temperatures ranging from 1 to 100 eV.

Understanding the mechanisms of WDP generation near the surface of active solar cell components may ultimately pave the way for future advancements in satellite infrastructure. By studying the development of WDPs, designs that are less susceptible to damage from a nuclear event may be created. In order to further the understanding of WDP generation, particularly with regards to the system of interest in this body of work, more variables may need to be considered in future work. One of these considerations should be towards the analysis of the propagation of the internal shockwave present within the target geometry during X-ray exposure. Another

variable of interest in future work is in studying what occurs at the interfaces between layers and sublayers of the solar panel infrastructure. By using more complex models for the system target geometry within the MD simulation, a greater understanding of the scope of the damage may be achieved as well as shedding light on possible weaknesses within the system's design.

Author's Presentations

1. Wenzel H. and G Miloshevsky. *Spatio-Temporal Evolution of Warm Dense Plasmas: Molecular Dynamics Modeling* Abstracts of the 23rd Annual Graduate Research Symposium, Virginia Commonwealth University, Richmond, VA, April 21, 2020.

2. Wenzel H. and G Miloshevsky. *Cold X-Ray Energy Deposition and Backscattering From Active Solar Cell Elements.* 2019 DTRA Radiation Effects Technical Review Ballston (Arlington), VA, June 25, 2019.

3. Wenzel H., M Fogleman, and G Miloshevsky. *Dynamics and Properties of High-Density Surface Plasmas Induced by Cold X-rays.* The 10-th International Workshop on Warm Dense Matter (WDM 2019), Travenmünde, Germany, May5 - 9, 2019.

4. Wenzel H. and G Miloshevsky. *Spectral Energy Distributions of Backscattered Photons and Electrons from Multi-layer Slab Targets.* Abstracts of the 22nd Annual Graduate Research Symposium, Virginia Commonwealth University, Richmond, VA, April 23, 2019, P13.

References

[1] Fogleman, Myles. Cold X-ray Effects on Satellite Solar Panels in Orbit. 2019. Web.

[2] Daligault, Jerome, and Travis Sjolstrom. "The Warm Dense Matter Regime." *Warm Dense Matter*, Los Alamos National Laboratory, www.lanl.gov/projects/dense-plasma-theory/background/warm-dense-matter.php.

[3] Varentsov, Dmitry. "Warm Dense Matter." *GSI*, 27 Mar. 2020, www.gsi.de/work/forschung/appamml/plasmaphysikphelix/experimente/warm_dense_matter.htm.

[4] "Warm Dense Matter." *HEDS*, SLAC National Accelerator Laboratory, 1 Nov. 2016, heds.slac.stanford.edu/our-research/warm-dense-matter.

[5] Daligault, Jerome, and Travis Sjolstrom. "The Physical Regimes." *Physical Regimes*, Los Alamos National Laboratory, www.lanl.gov/projects/dense-plasma-theory/background/physical-regimes.php.

[6] Nave, Carl R. "Compton Scattering." *Compton Scattering*, 2016, hyperphysics.phy-astr.gsu.edu/hbase/quantum/comptint.html.

[7] Lamarsh, John R., and Anthony Baratta. *Introduction to Nuclear Engineering.* Prentice Hall, 2009.

[8] "Overview." *geant4.Web.cern.ch*, CERN, 13 Mar. 2020, geant4.web.cern.ch/.

[9] Miloshevsky, Gennady. *Spatiotemporal Evolution of High-Density Surface Plasmas Produced by Prompt X-Rays*. DTRA Progress Report, June 2019.

[10] Ercolessi, Furio. "A molecular dynamics primer." *Spring college in computational physics, ICTP, Trieste* 19 (1997).

[11] Plimpton, Steve. "LAMMPS Molecular Dynamics Simulator." *LAMMPS Molecular Dynamics Simulator*, Sandia National Laboratories, lammps.sandia.gov/.

[12] Ji, Pengfei, and Yuwen Zhang. "First-principles Molecular Dynamics Investigation of the Atomic-scale Energy Transport: From Heat Conduction to Thermal Radiation." International Journal of Heat and Mass Transfer 60.C (2013): 69-80. Web.